Measuring radial flow of partonic and hadronic phases in relativistic heavy-ion collisions

Jajati K. Nayak and Jan-e Alam
Variable Energy Cyclotron Centre, 1/AF, Bidhan Nagar, Kolkata 700064, India
(Received 23 July 2009; published 11 December 2009)

It has been shown that the thermal photon and the lepton pair spectra can be used to estimate the radial velocity of different phases of the matter formed in nuclear collisions at ultrarelativistic energies. We observe a nonmonotonic variation of the flow velocity with invariant mass of the lepton pair, which is indicative of two different thermal dilepton sources at early and late stages of the dynamically evolving system. We also show that the study of radial velocity through electromagnetic probes may shed light on the nature of the phase transition from hadrons to a quark-gluon plasma.

DOI: 10.1103/PhysRevC.80.064906 PACS number(s): 25.75.Dw, 24.85.+p

I. INTRODUCTION

The numerical simulation of the QCD equation of state (EoS) predicts that nuclear matter at high density and/or temperature is composed of quarks and gluons owing to asymptotic freedom and screening of color charges [1–3]. Enormous experimental efforts have been made to produce such a partonic state of matter, called quark-gluon plasma (QGP), by colliding nuclei at ultrarelativistic energies. Careful theoretical investigations have been performed to understand the existing experimental data [4] and predictions for the forthcoming experiments [5] have also been made.

The hot and dense matter formed in the partonic phase after ultrarelativistic heavy-ion collisions expands in space and time owing to high internal pressure. Consequently, the system cools and reverts back to hadronic matter from the partonic phase. Initially (when the thermal system is just born) the entire energy of the system is thermal in nature and, with the progress of time, some part of the thermal energy gets converted to the collective (flow) energy. In other words, during the expansion stage, the total energy of the system is shared by the thermal as well as collective degrees of freedom. The evolution of the collectivity within the system is sensitive to the EoS. Therefore, the study of the collectivity in the system formed after nuclear collisions will be useful to shed light on the EoS [6–8] of the strongly interacting system at high temperatures and densities.

It is well known that the average magnitude of radial flow can be extracted from the transverse momentum (p_T) spectra of the hadrons. However, hadrons, being strongly interacting objects, can provide information on the state of the system when it is too dilute to support collectivity. On the other hand, electromagnetic (EM) probes, that is, photons and dileptons, are produced and emitted from each space-time point. Therefore, estimating radial flow from the EM probes will shed light on the time evolution of the collectivity in the system. This was demonstrated by the NA60 Collaboration [9] through dilepton measurements in In + In collisions at Super Proton Synchrotron (SPS) energy. The slope of the transverse mass spectrum of lepton pairs, $T_{\rm eff}$, of invariant mass M can be related to the space-time averaged quantities such as radial flow velocity v_r and temperature $T_{\rm av}$ as $T_{\rm eff} \sim T_{\rm av} + M v_r^2$. The effective temperature $T_{\rm eff}$ estimated from dilepton spectra [9] shows a different kind of behavior [10–15] compared with that from hadronic spectra. The effective temperature extracted from transverse mass spectra of dileptons increases linearly with invariant mass M up to ρ peak and then falls (but the PHENIX data do not show this trend [16]). In a recent work [17], we have shown that the ratio ($R_{\rm em}$) of the p_T spectra of photons to lepton pairs has an advantage over the individual spectra because some of the uncertainties or model dependence pertaining to the individual spectra get canceled in the ratio. Hence the ratio can be used as an efficient tool to understand the state of an expanding system. In the present work, we focus on the extraction of the radial flow from $R_{\rm em}$. We also argue that the simultaneous measurements of photons and dileptons will enable us to estimate the value of v_r for various invariant mass windows of the lepton pairs. The v_r values obtained from the analysis of both the spectra vary with M nonmonotonically. Such a behavior may be interpreted as being due to the presence of two different kinds of thermal sources of lepton pairs of the expanding system.

The paper is organized as follows. In Sec. II the ratio of thermal photon and dilepton productions is discussed. In Sec. III the evolution dynamics of the hot fireball system with specific initial conditions and EoS is outlined. The discussions in Secs. II and III are very brief as the details are available elsewhere [17]. The results are presented in Sec. IV. Finally Sec. V is devoted to a summary.

II. ELECTROMAGNETIC PROBES

The ratio $R_{\rm em}$ of the p_T spectra of thermal photons to dileptons can be written as follows [17]:

$$R_{\rm em} = \frac{\frac{d^2N_\gamma}{d^2p_Tdy}}{\frac{d^2N_\gamma^*}{d^2p_Tdy}} = \frac{\sum_i \int_i \left(\frac{d^2R_\gamma}{d^2p_Tdy}\right)_i d^4x}{\sum_i \int_i \left(\frac{d^2R_{\gamma^*}}{d^2p_Tdy dM^2}\right)_i dM^2 d^4x}. \quad (1)$$

The numerator (denominator) is the invariant momentum distribution of the thermal photons (lepton pairs). In Eq. (1) p_T, y, and M denote the transverse momentum, rapidity, and the invariant mass of the lepton pair, respectively. The summation in Eq. (1) runs over all phases through which the system passes during the expansion. ($d^2R/d^2p_Tdy_i$) and

$(d^2R/d^2p_T dy dM_i^2)$ are the static rates of photon and dilepton productions from the phase i, which is convoluted over the expansion dynamics through the space-time integration over d^4x. The integration over M is done by selecting appropriate invariant mass windows—$M_{\rm min} \leqslant M \leqslant M_{\rm max}$—and we define $\langle M\rangle = (M_{\rm min} + M_{\rm max})/2$.

The rate of thermal dilepton production per unit space-time volume per unit four-momentum volume is given by [18–21]

$$\frac{dR}{d^4p} = \frac{\alpha}{12\pi^4 p^2} L(p^2) {\rm Im}\Pi^{R\mu}_{\mu} f_{\rm BE}, \quad (2)$$

where α is the EM coupling constant, ${\rm Im}\Pi^{\mu}_{\mu}$ is the imaginary part of the retarded photon self-energy, and $f_{\rm BE}(E,T)$ is the thermal phase space factor for bosons. $L(p^2) = (1 + \frac{2m^2}{p^2})\sqrt{1-4\frac{m^2}{p^2}}$ arises from the final-state leptonic current involving Dirac spinors of mass m. The real photon production rate can be obtained from the dilepton emission rate by replacing the product of EM vertex $\gamma^\star \to l^+l^-$, the term involving final-state leptonic current, and the square of the (virtual) photon propagator by the polarization sum for the real photon. For an expanding system E should be replaced by $u_\mu p^\mu$, where p^μ and u^μ are the four-momentum and the four-velocity, respectively.

A. Thermal photons

The photon production rate has been evaluated by various authors [22] using hard thermal loop [23] approximations. The complete calculation of emission rate of photons from QGP to order $O(\alpha, \alpha_s)$ has been done by resuming ladder diagrams in effective theory [24]. This rate of production has been considered in the present work. A set of hadronic reactions with all isospin combinations has been considered for the production of photons [25–27] from hadronic matter. The effect of hadronic dipole form factors has been taken into account in the present work. We have checked that the high-p_T (∼2–3 GeV) part of the thermal photon spectra is dominated by the contributions from the QGP phase for a large initial temperature.

B. Thermal dileptons

The lowest order process producing lepton pairs is q and $\bar{q}$ annihilation. For a finite-temperature QCD plasma, the correction of order $\alpha_s\alpha^2$ to the lowest order rate of dilepton production has been calculated in Refs. [28,29], which is considered in the present work. For the low-M dilepton production from the hadronic phase we consider the decay of light vector mesons ρ, ω, and ϕ as considered in Ref. [17]. The continuum part of the vector meson spectral functions has been included in the present work [30,31].

It is well known that the contributions from the QGP phase dominate the M spectra of the lepton pairs below the ρ peak and above the ϕ peak if no thermal effects of the spectral functions of the vector mesons (see Refs. [30,32,33] for review) are considered.

III. EVOLUTION DYNAMICS

In the collision of two energetic heavy ions a large amount of energy is dumped into a small volume. The space-time evolution of the matter has been studied using ideal relativistic hydrodynamics [34] with longitudinal boost invariance [35] and cylindrical symmetry. The initial energy density $[\epsilon(\tau_i, r)]$ and radial velocity $[v(\tau_i, r)]$ profiles are the same as in our earlier studies [17]. The value of transition temperature T_c is taken as 192 MeV as obtained in lattice QCD calculations [36], although a much lower value of T_c is also predicted in Ref. [37]. However, we have found that the dependence of $R_{\rm em}$ on T_c is weak. In a first-order phase transition scenario we use a bag EoS for the QGP phase and, for the hadronic phase, all the resonances with mass $\leqslant$2.5 GeV have been considered [38].

In the present work we have considered the initial and freeze-out conditions that reproduced the hadrons [39], the photon [40], and dilepton spectra for Relativistic Heavy Ion Collider (RHIC) energy [41]. The values of initial thermalization time, $\tau_i = 0.2$ fm/c, initial temperature $T_i = 400$ MeV, and the freeze-out temperature $T_F = 120$ MeV, have been taken as the input for the calculation. For the Large Hadron Collider (LHC) we have taken $T_i = 700$ MeV and $\tau_i = 0.08$ fm/c, which gives the hadron multiplicity $dN/dy = 2100$ [5].

IV. RESULTS AND DISCUSSION

In Fig. 1 the photon and dilepton spectra have been displayed for RHIC conditions. Results indicate that the photon spectra from QGP dominate over their hadronic counterparts for $p_T > 1.5$ GeV. The dilepton from QGP and hadrons are comparable in magnitude for the entire range of p_T for $M \sim 1.2$ GeV (which is because of the inclusion of the continuum of the vector meson spectral functions [30,31]; without the continuum the quark matter part dominates). However, for $M \sim 0.75$ GeV, the dileptons from the hadronic matter are overwhelmingly large compared with quark matter contributions (not shown in the figure). Therefore, an

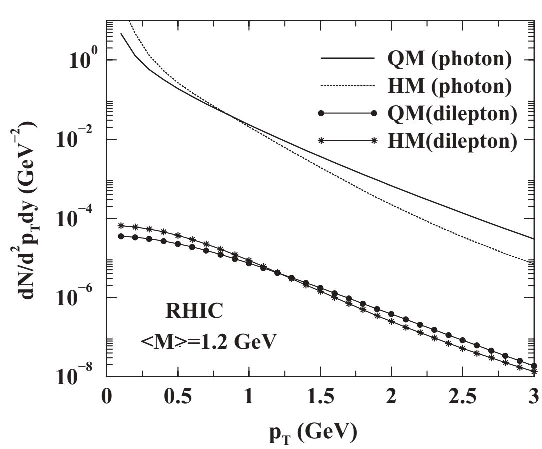

FIG. 1. The p_T spectra of photons and dileptons from hadronic and quark matter at RHIC energy. The dilepton spectra are obtained by integrating M from $M = 1.0$ to 1.4 GeV.

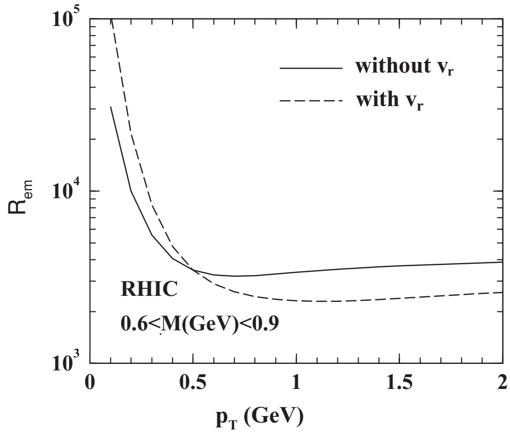

FIG. 2. $R_{\rm em}$ as a function of p_T with and without radial flow for invariant mass $0.6 < M$ (GeV) < 0.9. The spectrum with radial flow is normalized to the one without radial flow at $p_T = 0.5$ GeV.

appropriate selection of p_T and M will be very useful to characterize a particular phase of the system.

Now we consider the variation of the ratio $R_{\rm em}$ as a function of p_T for different invariant mass windows. The results are shown in Figs. 2 and 3. The variation of $R_{\rm em}$ with respect to p_T can be parametrized as follows:

$$R_{\rm em} \equiv A_3 \left(\frac{m_T}{p_T}\right)^{B_3} \exp[C_3(m_T - p_T)], \tag{3}$$

where A_3, B_3, and C_3 are constants and M_T, the transverse mass of the lepton pair, is defined as $M_T = \sqrt{p_T^2 + M^2}$. It is observed that the ratio decreases sharply and reaches a plateau beyond $p_T > 1.5$ GeV. This behavior of $R_{\rm em}$ as a function of p_T can be understood as follows: (i) For $p_T \gg M$, $M_T \sim p_T$ and consequently $R_{\rm em} \sim A_3$, giving rise to a plateau at large p_T. The height of the plateau is sensitive to the initial temperature of the system [17]. (ii) For $p_T < M$, $R_{\rm em} \sim \exp(-p_T/T_{\rm eff})/p_T^{B_3}$, which indicates a decrease of the ratio with p_T (at low p_T) as observed in Figs. 2 and 3.

To indicate the effect of v_r we have evaluated $R_{\rm em}$ with and without radial flow (see Figs. 2 and 3). In the case of vanishing radial flow the ratio can be parametrized as follows:

$$R^1_{\rm em} \equiv A_1 \left(\frac{m_T}{p_T}\right)^{B_1} \exp[C_1(m_T - p_T)]. \tag{4}$$

Here C_1 contains the information of the average temperature $T_{\rm av}$ of the system.

In the case of vanishing radial flow velocity the inverse slope of the photon and dilepton spectra represent the average temperature $T_{\rm av}$ of the system. However, in the case of nonzero radial flow the inverse slope contains the effect of average temperature as well as that of v_r. Therefore, the difference in the slopes of the two cases will enable us to estimate the amount of collectivity in the system.

As mentioned before for large initial temperature the transverse momentum distribution of photons from QGP dominates over its hadronic counterpart for $p_T \geqslant 1.5$ GeV. However, in the case of dileptons one has to select both the M and the p_T windows to observe QGP. For example, the thermal dileptons from hadrons dominate over those from QGP for $M \sim 0.75$ GeV. Therefore, for estimating the radial velocity in the hadronic phase we chose $p_T \sim 0.5$ GeV and $M \sim 0.75$ GeV for demonstrative purposes. Similarly, p_T and M windows may be selected where contributions from QGP dominate.

The exponential slope of the ratio C_3 can be related to the individual slopes of photons, $T^{-1}_{\rm eff1}$, and dileptons, $T^{-1}_{\rm eff2}$, as follows:

$$C_3 \times (m_T - p_T) = \frac{m_T}{T_{\rm eff2}} - \frac{p_T}{T_{\rm eff1}},$$

Writing the effective (blue-shifted) temperatures of the photon spectra and dilepton spectra as

$$T_{\rm eff1} = T_{\rm av}\sqrt{\frac{(1+v_r)}{(1-v_r)}}, \qquad T_{\rm eff2} = T_{\rm av} + M{v_r}^2, \tag{5}$$

we obtain

$$C_3 \times (m_T - p_T) = \frac{m_T}{T_{\rm av} + M{v_r}^2} - \frac{p_T}{T_{\rm av}\sqrt{(1+v_r)/(1-v_r)}}.$$

Further simplification leads to

$$aT^2_{\rm av} + bT_{\rm av} + c = 0, \tag{6}$$

where a, b, and c are functions of v_r. Solving Eq. (6) for a given C_3, M, and p_T we obtain v_r as a function of the average temperature. The results are displayed in Figs. 4 and 5 for initial conditions of RHIC and LHC energies for invariant mass and p_T windows indicated. The contributions in the M and p_T windows shown in Fig. 4 are dominated by the hadronic phase, that is, from the temperature range $T_c \sim 192$ MeV to $T_F \sim 120$ MeV. The radial velocity increases sharply with decreasing $T_{\rm av}$ in the hadronic phase.

We have evaluated v_r with a (continuous) EoS where the mixed phase does not appear. In this case v_r is larger than the one obtained for a strong first-order phase transition (Fig. 4), which indicates that the presence of the mixed phase (of hadrons and QGP) characterized by zero sound velocity slowed

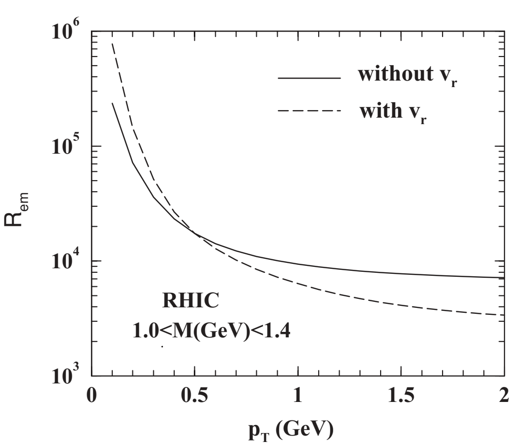

FIG. 3. $R_{\rm em}$ as a function of p_T as in the previous figure for invariant mass $1.0 < M$ (GeV) < 1.4.

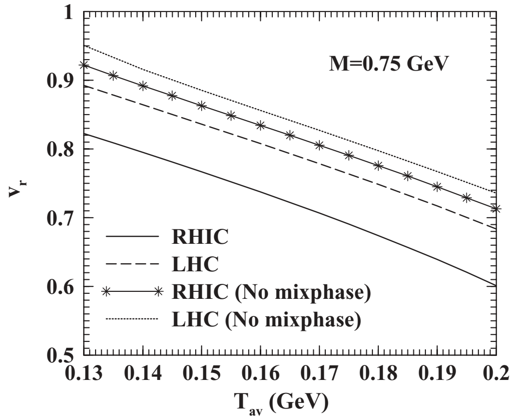

FIG. 4. Variation of v_r with T_{av} for $M = 0.75$ GeV and $p_T = 0.5$ GeV. The solid (dashed) line indicates the results for RHIC (LHC) for an EoS with a first-order phase transition. The line with asterisks (dotted line) stands for RHIC (LHC) for an EoS that excludes the mixed phase.

down the expansion of the system, resulting in a lower radial flow. Therefore, extraction of v_r from experimental data will be useful to understand the nature of the transition.

In Fig. 5 the radial velocity is displayed for the (average) temperature range that is dominated by the QGP phase. The results indicate a moderate v_r for RHIC but a large v_r is achieved even in the QGP phase for LHC energies; in fact, a fast increase in v_r is observed for T_{av} close to the transition temperature in the case of LHC. The value of v_r for LHC is much larger than for RHIC because of the longer lifetime and larger internal pressure of the partonic phase in LHC than in RHIC.

In a first-order phase transition scenario the QGP formed in heavy-ion collisions returns back to hadrons through a first-order phase transition. The temperature changes continuously from T_i to T_F. We estimate the average values of the radial velocity $v_{\rm isoth}$ on the constant temperature surfaces determined by the conditions: $T(r,\tau) = T_S$, for various values of T_S. The variation of $v_{\rm isoth}$ with T_S is depicted in Fig. 6 for both

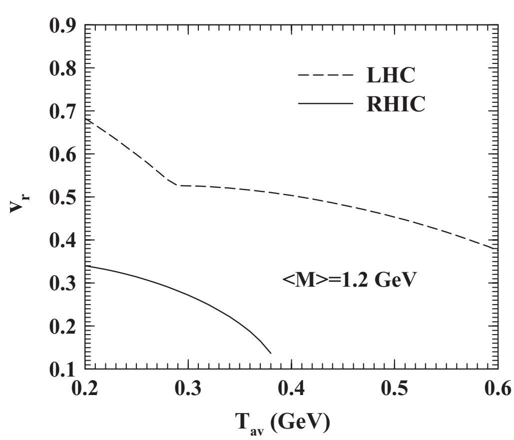

FIG. 5. Variation of v_r with T_{av} for $M = 1.2$ GeV and $p_T = 0.5$ GeV at RHIC and LHC energies for an EoS with a first-order phase transition.

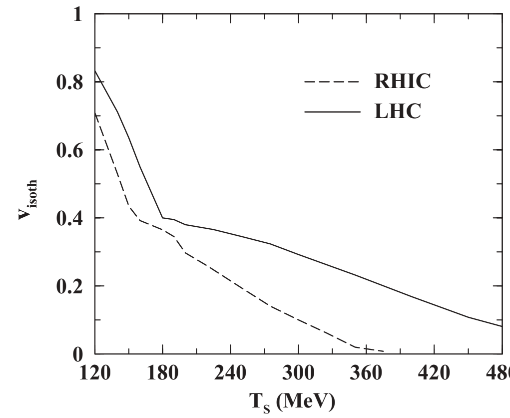

FIG. 6. Variation of average radial velocity of the fluid on a constant-temperature surface.

RHIC and LHC energies. $v_{\rm isoth}$ for LHC is larger than for RHIC because of higher initial temperature and hence internal pressure. In contrast to the results shown in Figs. 4 and 5, the variation of $v_{\rm isoth}$ with T_S is not measurable as it does not depend on the kinematic variables, p_T and M. The expansion is slower in the hadronic phase because of the softer EoS compared with the QGP phase. For given T_c and T_F the lifetime of the hadronic phase is larger for softer EoS, allowing the system to develop large radial flow, as evident from the results depicted in Fig. 6 for the low-temperature part. The effective temperature extracted from the ratio is displayed in Fig. 7 as a function of M for RHIC energy. $T_{\rm eff}$ increases with M up to the ρ peak and then decreases beyond ρ mass. The reduction of $T_{\rm eff}$ beyond ρ indicates the dominance of the radiation from the high-temperature phase in the high-M region. For LHC, however, no clear reduction of $T_{\rm eff}$ beyond the ρ peak is observed (Fig. 8). At LHC the average temperature and the flow velocity in the early phase (from where high-M pairs originate) are large (see Fig. 4). Hence the combination of both large v_r and large $T_{\rm av}$ does not allow $T_{\rm eff}$ to fall above the

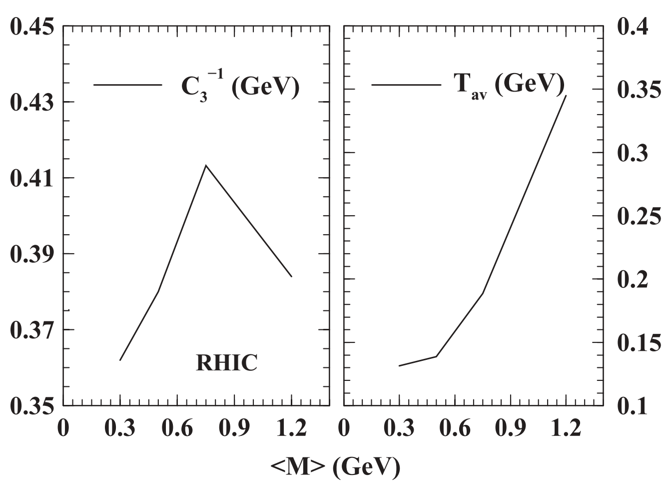

FIG. 7. Left: The variation of the slope C_3 with invariant mass obtained from the p_T spectra ratio for RHIC energy. Right: The variation of average temperature of the system. The left (right) vertical label is for the left (right) panel.

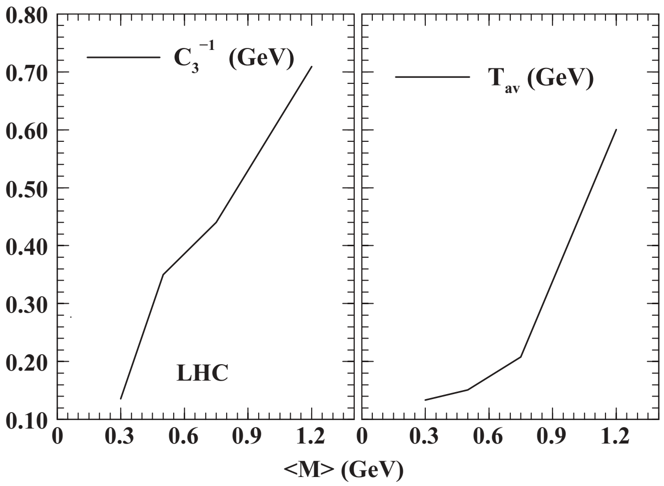

FIG. 8. The variation of the slope C_3 with invariant mass obtained from the p_T spectra ratio for LHC. Note that the scales in the left and right panels are the same.

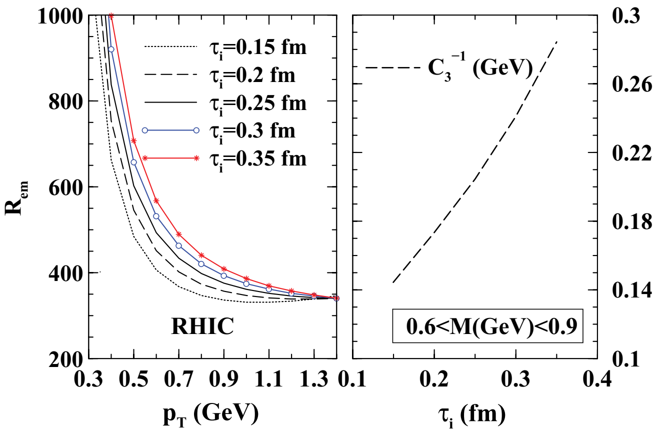

FIG. 10. (Color online) Left: Ratio of the p_T spectra for different initial thermalization times τ_i with all other parameters kept the same. Right: Variation of the effective slope C_3 as a function of initial thermalization time τ_i. The left (right) vertical label is for the left (right) panel.

ρ peak. The dependence of individual spectra on T_F is quite strong; however, we have observed that the slope of the ratio is insensitive to T_F and also to T_c. The slope of the ratio does not change when parameters such as T_F change from 0.120 to 0.150 GeV and T_c from 0.192 to 0.175 GeV.

Eliminating $T_{\rm av}$ from Eq. (5) and taking the values of $T_{\rm eff1}$ and $T_{\rm eff2}$ from photon and dilepton spectra one can obtain the variation of v_r as a function of M. The results are shown in Fig. 9 for RHIC and LHC energies. A nonmonotonic behavior of v_r with M is observed. A similar nonmonotonic behavior is observed in the elliptic flow (v_2) of photons as a function of transverse momentum [42,43]. Comparison of dilepton production from QGP and hadronic sources [17] indicates that in the low-M ($<m_\rho$) and high-M ($>m_\phi$) regions the emission rate from QGP dominates over its hadronic counterpart if the medium effects on the vector meson spectral functions are neglected. In other words, for a dynamically evolving system, the low- and high-M pairs are emitted from the early QGP phase, whereas lepton pairs with M around ρ mass

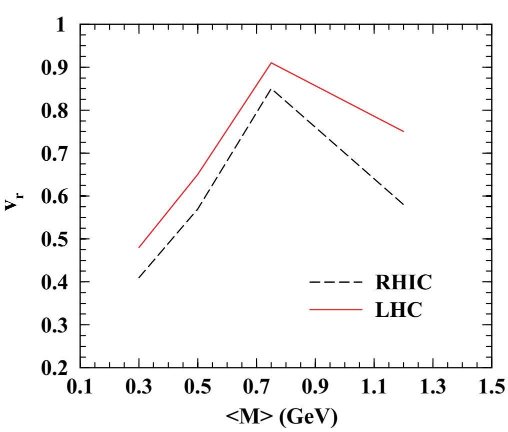

FIG. 9. (Color online) Radial velocity as a function of M for RHIC and LHC energies.

are emitted from the late hadronic phase. Therefore, low- and high-M domains represent early time—where $v_{\rm r}$ is low—and the $M \sim m_\rho$ domain represents late time—where $v_{\rm r}$ is large—giving rise to the observed variation in Fig. 9, which is indicative of two different kinds of source in early and late times of the evolving system. For $M \sim 1.2$ GeV the flow velocity is not very small since this window is populated by both hadronic and partonic contributions almost equally. Again, at LHC energy, the partonic phase lifetime is greater, which favors the development of larger flow compared with RHIC energy. It is important to note at this point that for LHC, although the slope C_3 does not show a clear nonmonotonic behavior with M, v_r does. This is because, as described before, the slope C_3 depends not only on v_r but also on $T_{\rm av}$ and both are large in the partonic phase at LHC.

The two time scales, namely, the lifetime of the partonic phase ($\tau_{\rm QGP}$) and the time an inward-moving rarefaction wave takes to hit the center of the cylindrical geometry, decide whether radial flow plays an important role in the partonic phase. The latter time scale is defined as $\tau_{\rm rw} \sim R/c_s$ where R is the transverse size of the system and c_s is the velocity of sound. If $\tau_{\rm QGP} \sim \tau_{\rm rw}$ then v_r will be large in the partonic phase. Therefore, an increase in τ_i ($\tau_{\rm QGP} \propto \tau_i$) will increase the radial flow in the partonic phase if the initial and the critical temperatures are kept fixed. However, an increase in τ_i from τ_1 to τ_2 produces the same flow if T_i decreases by a factor of $(\tau_2/\tau_1)^{1/3}$. For a fixed T_i an increase in τ_i will increase the effective slope as evident from the right panel of Fig. 10. Therefore, the slope of the ratio may be used effectively to estimate the value of initial thermalization time.

V. SUMMARY

It has been shown that the p_T distribution of thermal photons and lepton pair spectra may be used simultaneously to estimate the magnitude of the radial velocity of different phases of the matter formed in nuclear collisions at ultrarelativistic energies. Judicious choices of the kinematic variables, for example, the invariant mass and the transverse momentum windows may be selected to estimate the flow velocity in the partonic and hadronic phases of the evolving matter. It has been observed that for RHIC and LHC energies the flow velocity increases with invariant mass up to the ρ peak, beyond which it decreases. The $T_{\rm eff}$ may not decrease with mass beyond the ρ peak if the average temperature and the flow velocity are large in the partonic phase as in the case of LHC energy. By doing a simple analysis of photon and dilepton spectra we have extracted the radial flow velocity for various invariant mass windows. v_r varies with M nonmonotonically. We argue that such a variation indicates the presence of two different types of thermal sources of lepton pairs.

ACKNOWLEDGMENTS

JA is supported by DAE-BRNS Project Sanction No. 2005/21/5-BRNS/2455.

[1] J. C. Collins and M. J. Perry, Phys. Rev. Lett. **34**, 1353 (1975).
[2] M. B. Kislinger and P. D. Morley, Phys. Rev. D **13**, 2765 (1976); **13**, 2771 (1976).
[3] E. V. Shuryak, Phys. Rep. **61**, 71 (1980); **115**, 151 (1984).
[4] J. Alam, S. Chattopadhyay, T. Nayak, B. Sinha, and Y. P. Viyogi (eds.), J. Phys. G **35** (2008) (Proc. Quark Matter 2008).
[5] N. Armesto *et al.*, J. Phys. G **35**, 054001 (2008).
[6] E. Schnedermann, J. Sollfrank, and U. Heinz, Phys. Rev. C **48**, 2462 (1993).
[7] C. M. Hung and E. Shuryak, Phys. Rev. C **57**, 1891 (1998).
[8] T. Hirano and K. Tsuda, Phys. Rev. C **66**, 054905 (2002).
[9] R. Arnaldi *et al.* (NA60 Collaboration), Phys. Rev. Lett. **100**, 022302 (2008); S. Damjanovic (NA60 Collaboration), J. Phys. G **35**, 104036 (2008).
[10] H. van Hees and R. Rapp, Phys. Rev. Lett. **97**, 102301 (2006).
[11] H. van Hees and R. Rapp, Nucl. Phys. **A806**, 339 (2008).
[12] J. Ruppert, C. Gale, T. Renk, P. Lichard, and J. I. Kapusta, Phys. Rev. Lett. **100**, 162301 (2008).
[13] T. Renk and J. Ruppert, Phys. Rev. C **77**, 024907 (2008).
[14] K. Dusling and I. Zahed, Phys. Rev. C **80**, 014902 (2009).
[15] J. Alam, T. Hirano, J. K. Nayak, and B. Sinha, arXiv:0902.0446 [nucl-th].
[16] A. Toia (PHENIX Collaboration), J. Phys. G **35**, 104037 (2008).
[17] J. K. Nayak, J. Alam, S. Sarkar, and B. Sinha, Phys. Rev. C **78**, 034903 (2008).
[18] L. D. McLerran and T. Toimela, Phys. Rev. D **31**, 545 (1985).
[19] C. Gale and J. I. Kapusta, Nucl. Phys. **B357**, 65 (1991).
[20] H. A. Weldon, Phys. Rev. D **42**, 2384 (1990).
[21] J. Alam, S. Raha, and B. Sinha, Phys. Rep. **273**, 243 (1996).
[22] J. Kapusta, P. Lichard, and D. Seibert, Phys. Rev. D **44**, 2774 (1991); R. Bair, H. Nakkagawa, A. Niegawa, and K. Redlich, Z. Phys. C **53**, 433 (1992); P. Aurenche, F. Gelis, H. Zaraket, and R. Kobes, Phys. Rev. D **58**, 085003 (1998).
[23] E. Braaten and R. D. Pisarski, Nucl. Phys. **B337**, 569 (1990); **B339**, 310 (1990).
[24] P. Arnold, G. D. Moore, and L. G. Yaffe, J. High Energy Phys. 11 (2001) 057; 12 (2001) 009; 06 (2002) 030.
[25] S. Sarkar, J. Alam, P. Roy, A. K. Dutt-Mazumder, B. Dutta-Roy, and B. Sinha, Nucl. Phys. **A634**, 206 (1998).
[26] P. Roy, S. Sarkar, J. Alam, and B. Sinha, Nucl. Phys. **A653**, 277 (1999).
[27] S. Turbide, R. Rapp, and C. Gale, Phys. Rev. C **69**, 014903 (2004).
[28] T. Altherr and P. V. Ruuskanen, Nucl. Phys. **B380**, 377 (1992).
[29] M. H. Thoma and C. T. Traxler, Phys. Rev. D **56**, 198 (1997).
[30] J. Alam, S. Sarkar, P. Roy, T. Hatsuda, and B. Sinha, Ann. Phys. (NY) **286**, 159 (2000).
[31] E. V. Shuryak, Rev. Mod. Phys. **65**, 1 (1993).
[32] G. E. Brown and M. Rho, Phys. Rep. **269**, 333 (1996).
[33] R. Rapp and J. Wambach, Adv. Nucl. Phys. **25**, 1 (2000).
[34] H. von Gersdorff, L. D. McLerran, M. Kataja, and P. V. Ruuskanen, Phys. Rev. D **34**, 794 (1986).
[35] J. D. Bjorken, Phys. Rev. D **27**, 140 (1983).
[36] M. Cheng *et al.*, Phys. Rev. D **74**, 054507 (2006).
[37] Y. Aoki, Z. Fodor, S. D. Katz, and K. K. Szab, Phys. Lett. **B643**, 46 (2006).
[38] B. Mohanty and J. Alam, Phys. Rev. C **68**, 064903 (2003).
[39] B. K. Patra, J. Alam, P. Roy, S. Sarkar, and B. Sinha, Nucl. Phys. **A709**, 440 (2002).
[40] J. Alam, J K Nayak, P. Roy, A. K. Dutt-Mazumder, and B. Sinha, J. Phys. G **34**, 871 (2007).
[41] P. Mohanty *et al.* (in preparation).
[42] R. Chatterjee, E. S. Frodermann, U. Hienz, and D. K. Srivastava, Phys. Rev. Lett. **96**, 202302 (2006).
[43] F.-M. Liu, T. Hirano, K. Werner, and Y. Zhu, Nucl. Phys. **A830**, 587c (2009).